JOC The Journal of Organic Chemistry

Article

pubs.acs.org/joc

Insights into the Dual Activation Mechanism Involving Bifunctional Cinchona Alkaloid Thiourea Organocatalysts: An NMR and DFT Study

Jun-Ling Zhu,[†] Yong Zhang,[†] Chong Liu,[†] An-Min Zheng,[‡] and Wei Wang*[,†]

[†]State Key Laboratory of Applied Organic Chemistry, College of Chemistry and Chemical Engineering, Lanzhou University, Lanzhou, Gansu 730000, China

[‡]State Key Laboratory of Magnetic Resonance and Atomic and Molecular Physics, Wuhan Center for Magnetic Resonance, Wuhan Institute of Physics and Mathematics, Chinese Academy of Sciences, Wuhan, Hubei 430071, China

Supporting Information

ABSTRACT: In-depth understanding of the activation mechanism in asymmetric organocatalysis is of great importance for rational development of highly efficient catalytic systems. In this Article, the mechanism for the direct vinylogous Michael reaction of α,β-unsaturated γ-butyrolactam (**Nu**) and chalcone (**EI**) catalyzed by the bifunctional cinchona alkaloid thiourea organocatalyst (**Cat**) was studied with a combination of experimental (NMR) and theoretical (DFT) approaches, through which a new dual activation pathway was found. The key feature of this new dual activation mechanism (Pathway C) is that one N−H_A of the thiourea moiety and the N−H of the protonated amine in **Cat** simultaneously activate **Nu**, while the other N−H_B of the thiourea moiety activates **EI**. Both the NMR measurement and the DFT calculation identified that the interaction of **Cat** with **Nu** is stronger than that with **EI** in the catalyst−substrate complexes. Kinetic studies via variable-temperature NMR measurements indicated that, with the experimental activation energy E_a of 10.2 kcal/mol, the reaction is all first-order in **Nu**, **EI**, and **Cat**. The DFT calculation further revealed that the C−C bond formation is both the rate-determining and the stereoselectivity-controlling steps. In agreement with the experimental data, the energy barrier for the rate-determining step along Pathway C was calculated as 8.8 kcal/mol. The validity of Pathway C was further evidenced by the calculated enantioselectivity (100% ee) and diastereoselectivity (60:1 dr), which are in excellent match with the experimental data (98% ee and >30:1 dr, respectively). Mechanistic study on the Michael addition of nitromethane to chalcone catalyzed by the **Catalyst I** further identified the generality of this new dual activation mechanism in cinchona alkaloid thiourea organocatalysis.

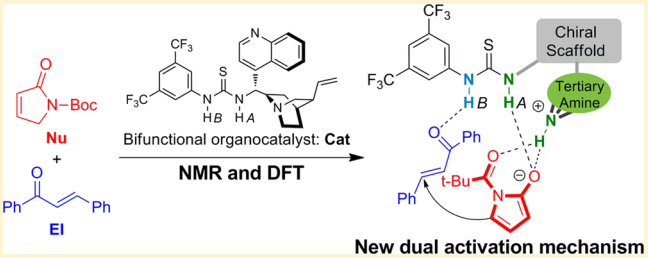

INTRODUCTION

Since 2000, asymmetric organocatalysis has been developed as a valuable strategy for the diverse synthesis of chiral compounds.[1] Design, application, and mechanistic investigation on new activation modes (such as enamine, iminium, and hydrogen-bonding catalysis) have dramatically advanced the development in this field.[2,3] Mimic to the enzyme catalysis, the bifunctional catalysis mode, that is, the simultaneous activation of two reaction substrates via multiple and relatively weak catalyst−substrate interactions (e.g., hydrogen bonding), has broadened the scope of research in asymmetric organocatalysis in recent years.[4,5] Particularly, the bifunctional thiourea−tertiary amine organocatalysts (Figure 1), bearing a thiourea moiety and an amine group in the chiral scaffold, have been used for catalyzing a variety of nucleophile−electrophile addition reactions.[4a,c−e,g,h,j,5] Although many synthetic achievements have been made with these bifunctional thiourea−tertiary amine organocatalysts, the mechanistic studies, especially on the activation modes, the elementary steps, and the origins of stereoselectivity control, have rarely been conducted via experimental approaches.[6] On the other hand, computational methods have been becoming a versatile tool for understanding the organocatalytic mechanisms toward the rational design of more efficient catalytic systems.[3g,7] In this context, several theoretical studies on bifunctional thiourea organocatalysis have been carried out, providing valuable insights into the catalytic mechanisms.[6d,e,8] For example, upon the first report of thiourea−tertiary amine organocatalysts, Takemoto et al.[6a,9] proposed a dual activation mechanism (Pathway A), in which the catalyst first

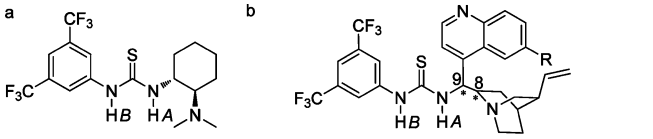

Figure 1. Typical bifunctional thiourea−tertiary amine organocatalysts: the Takemoto catalyst (a), and two representative examples of cinchona alkaloid thioureas (b).

Received: October 4, 2012
Published: October 8, 2012

deprotonates an acidic proton of the nucleophile, and then the thiourea activates the electrophile while the protonated amine activates the nucleophile. In contrast to the qualitative model proposed by Takemoto, Pápai et al.[8d] conducted theoretical studies and proposed an alternative dual activation mechanism (Pathway B). In Pápai's proposal, the thiourea activates the nucleophile, while the protonated amine activates the electrophile. Both Pathway A[8c,f,k,q,10] and Pathway B[8h,o,p,11] have found some validity in subsequent experimental and theoretical work. However, no systematic information is available about the preferential pathway for a certain reaction catalyzed by bifunctional thiourea–tertiary amine organocatalysts.

It is important to mention that even slight modification of the organocatalysts or substrates in the experimental protocols could significantly affect the yield and stereoselectivity of the reaction products.[12] On the other hand, adoption of the simplified catalysts or substrates to enhance the computational speed[8c,i–k] would also bring uncertainty to the theoretical elucidation of the real mechanisms involved in the complex thiourea–tertiary amine organocatalysis; this is especially true for predicting the stereoselectivity, which is more sensitive to the steric and electronic effects. Moreover, with the quinoline ring and the bulkier tertiary amine group (8-vinylquinuclidine) in the chiral scaffold, cinchona alkaloid thiourea organocatalysts (Figure 1b) are structurally different from that of the Takemoto catalyst (Figure 1a). Therefore, the reaction mechanism and the stereochemical control involved in cinchona alkaloid thiourea organocatalysis may also be different and more complex. However, examples of experimental or theoretical investigations on this important issue are rather rare.[8d,o]

We have recently developed an asymmetric direct vinylogous Michael addition of α,β-unsaturated γ-butyrolactam (**Nu**) with chalcone (**EI**) catalyzed by a cinchona alkaloid thiourea organocatalyst (**Cat** in Figure 1b).[13] The reaction was achieved with high yields (73–95%) and excellent enantio- and diastereoselectivities (94–99% ee and up to >40:1 dr). In this Article, we carried out mechanistic investigations on one representative example (Scheme 1) of this reaction via both

Scheme 1. Representative Example of the Asymmetric Direct Vinylogous Michael Addition of α,β-Unsaturated γ-Butyrolactam (Nu) to Chalcone (EI) Catalyzed by Bifunctional Cinchona Alkaloid Thiourea Organocatalyst (Cat)[13]

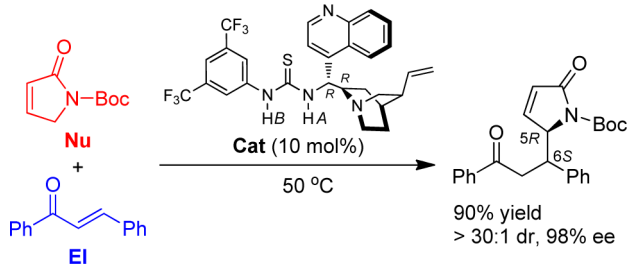

experimental (liquid ^{1}H NMR) and theoretical (DFT) approaches, through which a new dual activation mechanism (Scheme 3, Pathway C) was revealed. Different from those proposed by Takemoto (Pathway A) and Pápai (Pathway B), the binding mode in Pathway C is that one N–H_A of the thiourea moiety and the N–H of the protonated amine in **Cat** simultaneously activate **Nu**, while the other N–H_B of the thiourea moiety activates **EI**.

As shown in Figure 2, in the catalytic process of the investigated reaction, the catalyst (**Cat**) first activates both the enolic form of **Nu** (enolic **Nu**)[14] and **EI**, accompanied by the protonation of the quinuclidine amine of **Cat** (substrate binding and catalyst protonation). Through the formed ternary complex, the C–C bond formation occurs between **Nu** and **EI** (C–C bond formation). Afterward, the recovery of **Cat** and the formation of the reaction product are achieved via the dissociation and keto–enol tautomerization of the preliminary Michael adduct (catalyst recovery). In this Article, we accordingly clarified the following aspects concerning the reaction mechanism: (1) The interaction of **Cat** with **Nu** is stronger than that with **EI** in the catalyst–substrate complexes. (2) The C–C bond formation is both the rate-determining and the stereoselectivity-controlling step. (3) Most importantly, a new dual activation mode (Pathway C) was found for the C–C bond formation, in which one N–H_A of the thiourea moiety and the N–H of the protonated amine in **Cat** simultaneously activate **Nu**, while the other N–H_B of the thiourea moiety activates **EI**. (4) The activation energy and the stereoselectivity obtained via the DFT calculation are in excellent agreement with the experimental data, which validates Pathway C as the preferential activation mechanism. (5) Mechanistic study on the Michael addition of nitromethane to chalcone further verified the generality of Pathway C in cinchona alkaloid thiourea organocatalysis.

EXPERIMENTAL AND COMPUTATIONAL METHODS

^{1}H and ^{13}C NMR spectra of the catalyst (**Cat**), two substrates (**Nu** and **EI**), and the mixtures of **Cat** with **Nu** and **EI** were recorded at ambient temperature in either $CDCl_3$ or C_6D_6[15] on a 400 MHz liquid NMR spectrometer. Kinetic studies were performed through variable-temperature ^{1}H NMR measurements at T = 24, 30, 40, 50, and 60 °C with samples in NMR tubes using $CDCl_3$ as the solvent. The reaction order in **Nu** was determined by monitoring its consumption in the presence of a 10-fold excess of **EI**, while the reaction order in **EI** was examined in the same way with a 10-fold excess of **Nu**. The reaction order in **Cat** was determined by measuring the relative rate constant at different catalyst loadings.

The real structures of **Cat**, **Nu**, and **EI** were used in the computations without any simplification or modification. Solvent effect was also taken into account. Quantum chemical calculations were performed using the hybrid density functional method B3LYP[16] as implemented in the Gaussian 09 program suite.[17] All geometry structures were first optimized with the moderate 6-31G(d) basis set in the gas phase. A more accurate 6-31G(d,p) basis set was then employed for further optimization, using the CPCM polarization continuum model[18] and UFF radii, with $CHCl_3$ as the solvent. Afterward, frequency calculations were performed at the same level as the geometry optimizations to confirm the minimum and transition state (TS) structures (zero and only one imaginary frequency, respectively). Intrinsic reaction coordinates (IRC) were calculated for all of the transition states to verify that the saddle point has connected with the correct reactant and product on the potential energy surface.[19] Finally, single-point electronic energies were calculated with the B3LYP/6-311++G(d,p) including the solvent ($CHCl_3$) effect. Unless stated otherwise, the energy data are derived from the B3LYP/6-311++G(d,p) (CPCM, $CHCl_3$)//B3LYP/6-31G(d,p) (CPCM, $CHCl_3$) calculations, including the zero-point energy (ZPE) corrections from frequency calculation. The structure images were generated using CYLview software.[20] All of the bond lengths are in angstroms (Å), and the energies are in kcal/mol.

dx.doi.org/10.1021/jo302133n | J. Org. Chem. 2012, 77, 9813–9825

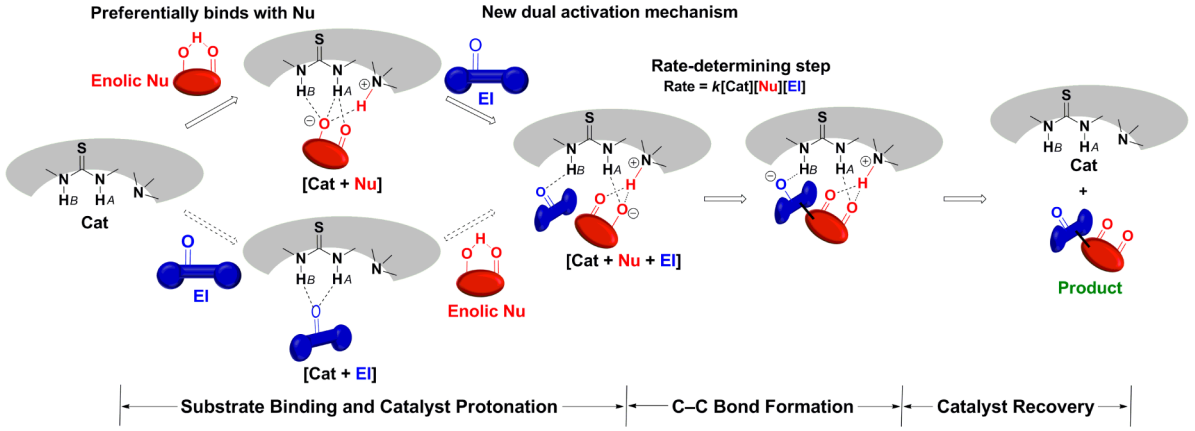

Figure 2. The catalytic process proposed for the reaction shown in Scheme 1, which involves a new dual activation mechanism. The key feature of this mechanism is that one N−H of the thiourea moiety and the N−H of the protonated amine in **Cat** simultaneously activate **Nu**, while the other N−H of the thiourea moiety activates **EI**.

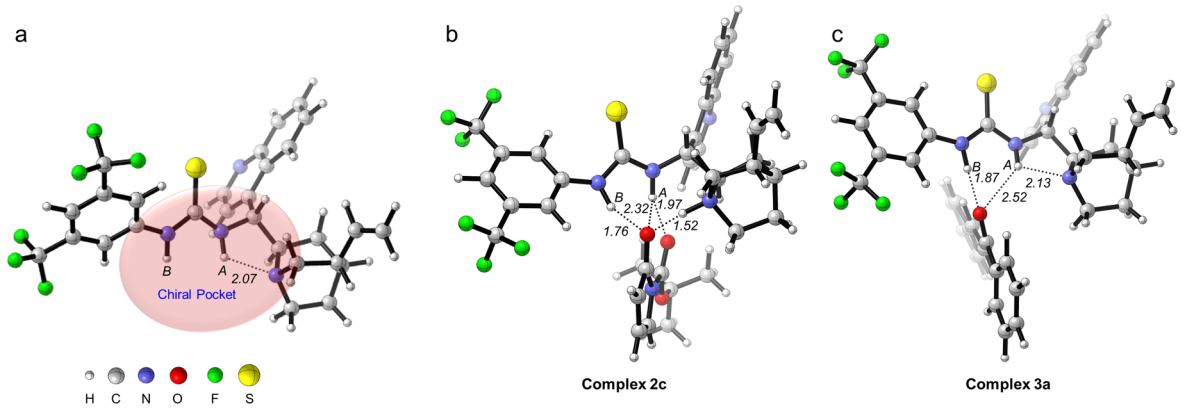

Figure 3. The most stable structures of **Cat** (a), **Cat**−**Nu** binary complex (b, **Complex 2c**), and **Cat**−**EI** binary complex (c, **Complex 3a**).

RESULTS AND DISCUSSION

Molecular Structure of the Catalyst. The bifunctional catalyst, **Cat**, was synthesized according to the published procedures.[21] The chemical structure of **Cat** was identified through a series of 1D and 2D NMR measurements, by which the ^{1}H and ^{13}C chemical shifts were fully assigned (Figures S1−4). **Cat** contains two active sites, that is, the thiourea moiety and the quinuclidine amine, in the chiral scaffold. Because the spatial arrangement of these two moieties is very important for activating the substrates, we first carried out the structure optimization to obtain the most stable conformation of **Cat**.[22] As depicted in Figure 3a, both the thiourea moiety and the quinuclidine amine orient to the same direction in the chiral scaffold of **Cat**. This conformation is ideal for the dual activation of both electrophiles and nucleophiles, and a similar result has previously been found with other **Cat** analogues.[6a,23] An intramolecular N−H···N hydrogen bond (length of 2.07 Å) is formed between the quinuclidine amine and one thiourea proton (N−H_A). These two active sites in the particular spatial arrangement, together with the quinoline ring and the quinuclidine moiety, provide uniquely a chiral active pocket (Figure 3a). This chiral pocket can efficiently bind and activate both substrates and, as a result, govern the stereoselectivity during the subsequent C−C coupling step (vide infra).

Substrate Binding and Catalyst Protonation. We applied both theoretical and experimental approaches to clarify how **Cat** activates **Nu** and **EI**. Via the DFT calculations, we succeeded in finding the most stable catalyst−substrate complexes. Via the ^{1}H NMR measurements, we were able to verify the hydrogen-bonding interaction between the catalyst and the substrates. Both the NMR measurement and the DFT calculation indicated that the interaction of **Cat** with **Nu** is stronger than that with **EI** in the catalyst−substrate complexes.

Theoretical calculations predicted that three stable binary **Cat**−**Nu** complexes (i.e., **Complex 1a**, **1b**, and **1c** in Scheme 2) can be first formed between **Cat** and the enolic **Nu** via the hydrogen bonds. The calculated binding energies of **Complex 1a**, **1b**, and **1c** are −0.2, −3.6, and −5.6 kcal/mol, respectively. The stability of these **Cat**−**Nu** complexes follows the order of **1a** < **1b** < **1c**, which is caused by the gradually enhanced hydrogen-bonding interaction between **Cat** and the enolic **Nu**. After the formation of the binary **Cat**−**Nu** complex, the quinuclidine amine of **Cat** deprotonates a proton from the enolic **Nu**, which is assisted by the adjacent thiourea N−H groups (Scheme 2). Because of the proton transfer, the interaction between **Nu** and **Cat** in the transiton states (i.e., $\mathbf{TS}_{1a-2a}$, $\mathbf{TS}_{1b-2b}$, and $\mathbf{TS}_{1c-2c}$ in Scheme 2) is increased as compared to that in the initial binary complexes (**Complex 1a**, **1b**, and **1c**). This makes the energy barrier of this process very low and even negative, the value of which is 1.4, −0.9, and −1.0 kcal/mol for **Complex 1a**, **1b**, and **1c**, respectively. This finding indicates that the protonation step is almost a barrierless process and, therefore, can easily proceed in each case. Similar cases have been identified in other proton-transfer reactions.[24]

dx.doi.org/10.1021/jo302133n | J. Org. Chem. 2012, 77, 9813−9825

Scheme 2. Formation of Three Cat−Nu Complexes and the Process of Cat Protonation

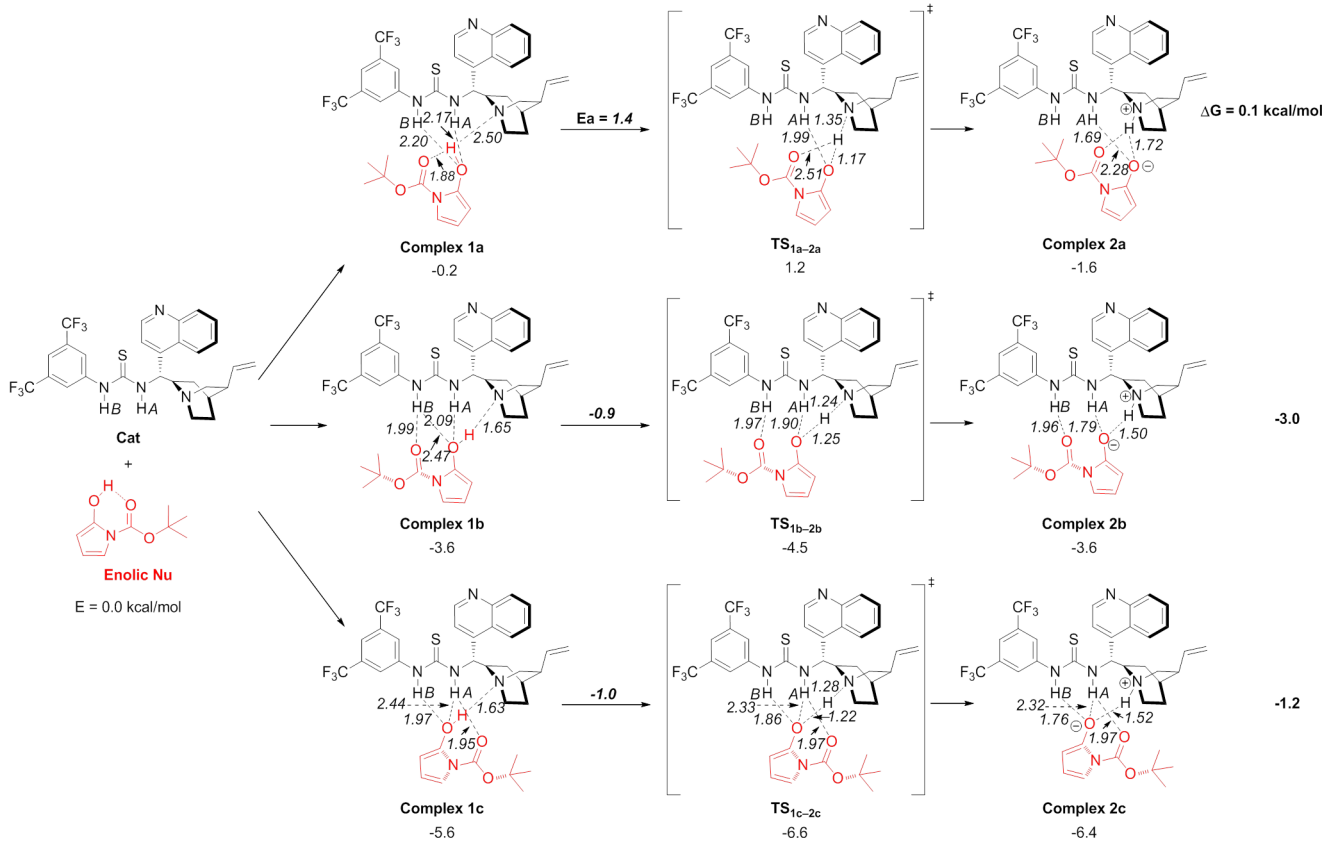

The interaction between **Nu** and **Cat** in the protonated binary complexes (i.e., **Complex 2a**, **2b**, and **2c** in Scheme 2) is stronger than that in the initial binary complexes (**Complex 1a**, **1b**, and **1c**), probably due to the zwitterion nature.[4e] **Complex 2c** is the most stable one, the final binding energy of which is −6.4 kcal/mol. As seen from the structure of **Complex 2c** (Scheme 2 and Figure 3b), **Nu** is activated by two N−H (N−H_A and N−H_B) of the thiourea moiety and one N−H of the protonated amine. Moreover, the changes (ΔG) in the Gibbs free energy for this process are also as low as 0.1, −3.0, and −1.2 kcal/mol, respectively.[25] Therefore, the protonation of **Cat** is kinetically feasible and thermodynamically reversible.

As shown in Figure 3c, our calculations indicated that, with a binding energy of −4.5 kcal/mol (see Supporting Information for details), the most stable binary **Cat**−**EI** complex (**Complex 3a**) is formed through two hydrogen bonds. In the binary **Complex 3a**, due to the strong steric repulsion between the two phenyl groups of **EI** and the quinuclidine moiety of **Cat**, **EI** is nearly perpendicular to the plane of the thiourea moiety of **Cat**. Two (one weak and one strong) hydrogen bonds (2.52 and 1.87 Å) can be formed between the carbonyl group of **EI** and the thiourea N−H_A, N−H_B of **Cat**, respectively. The binding energy of the binary **Cat**−**Nu** complex (**Complex 2c**, −6.4 kcal/mol) is 1.9 kcal/mol larger than that of the binary **Cat**−**EI** complex (**Complex 3a**, −4.5 kcal/mol). Therefore, the binding of **Cat** with **Nu** is stronger than that with **EI**.

The above results on substrate binding were further verified by our NMR investigations. Figure 4 shows the ^{1}H NMR spectra of **Cat** in the presence of **Nu** (from 0.0 to 3.0 equiv) in C_6D_6.[26] Almost all of the protons of **Cat** were shifted to downfield upon the addition of **Nu**, and the shifted values are approximately linear to the amount of **Nu**. In particular, N−H,[27] H3′, H2″, H9, H2, H5′, H6, and H8 of **Cat** were shifted more significantly than other protons. When **Cat** was mixed with 3.0 equiv of **Nu**, the downfield-shifted values for these protons were 0.71, 0.40, 0.38, 0.32, 0.26, 0.21, 0.20, and 0.16 ppm, respectively. Meanwhile, the protons of **Nu** were also shifted slightly to the downfield. The significantly shifted

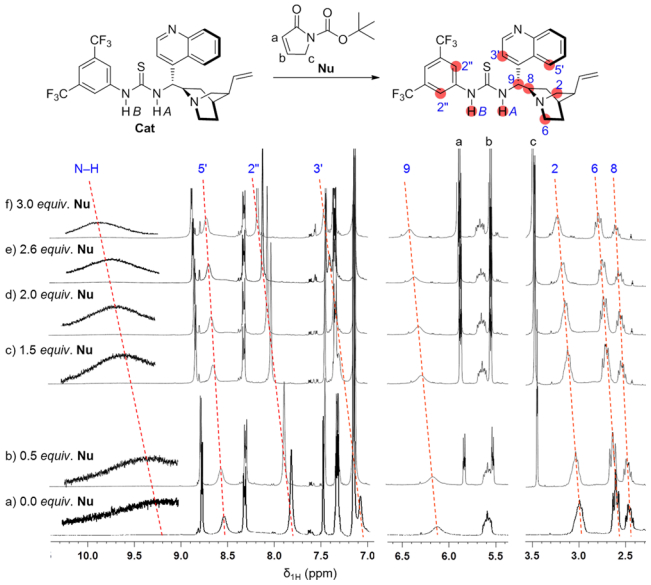

Figure 4. ^{1}H NMR spectra of **Cat** recorded in the presence of **Nu** in different amounts (from 0.0 to 3.0 equiv) in C_6D_6.[26] The **Cat** protons with significant change in their ^{1}H chemical shifts were marked in red for clarity.

dx.doi.org/10.1021/jo302133n | J. Org. Chem. 2012, 77, 9813−9825

T (K)	1/T (K^{-1})	k ($L \cdot mol^{-2} \cdot min^{-1}$)	lnk
297	0.0034	0.0011	-6.82
303	0.0033	0.0019	-6.29
313	0.0032	0.0030	-5.82
323	0.0031	0.0050	-5.30
333	0.0030	0.0073	-4.92

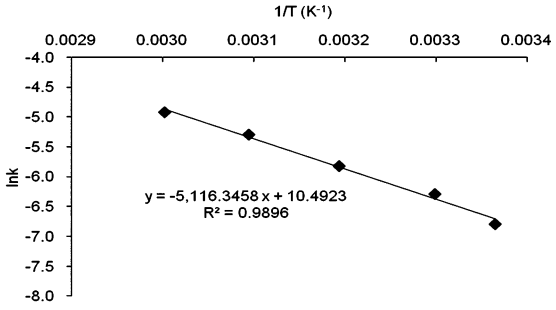

Figure 5. The rate constants k obtained at T = 24, 30, 40, 50, and 60 °C (left), and the Arrhenius plot for the reaction (right). The experimental activation energy E_a was determined as 10.2 kcal/mol.

Scheme 3. Possible Pathways for the Dual Activation Mechanism on the Formation of the Main Product (5*R*, 6*S*)[a]

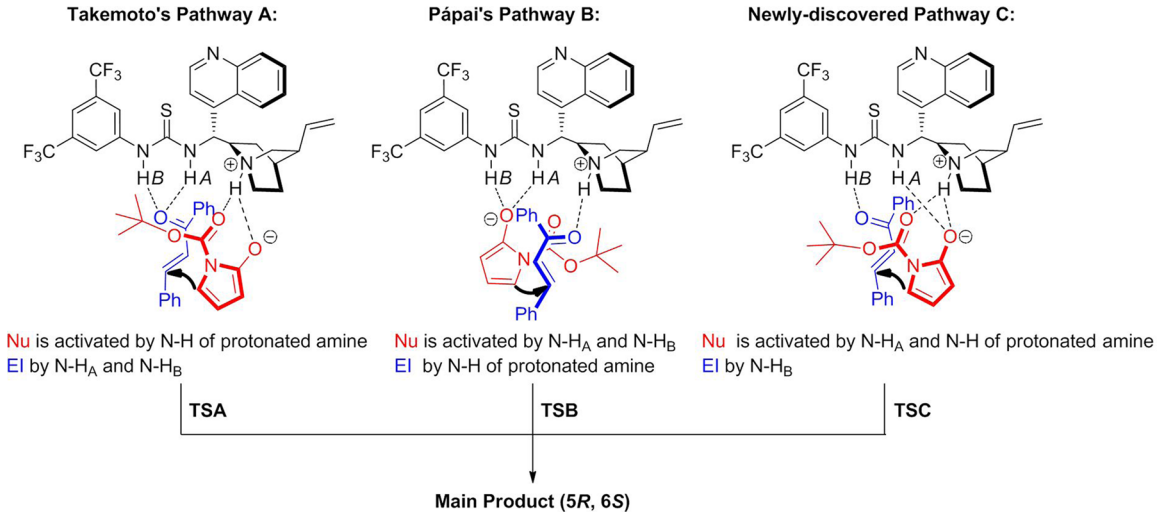

[a]Pathway C is the new dual activation mode found in this Article.

protons (marked in red in Figure 4) in **Cat** are around the N−H groups of the thiourea and the nitrogen atom of the quinuclidine, which indicates that **Cat** binds with **Nu** mainly through these two active sites. The results obtained from NMR investigations are well consistent with our theoretical calculations. In the most stable **Cat**−**Nu** complex (**Complex 2c**) predicted by theoretical calculations, stronger hydrogen bonds are formed between **Nu** and the thiourea N−H groups together with the protonated quinuclidine amine (vide supra).

On the contrary, when **Cat** was mixed with 3.5 equiv of **EI**, the thiourea N−H was shifted 0.16 ppm to downfield, while other protons in **Cat** and all protons in **EI** remained almost unchanged (Table S1). This result implied that **EI** mainly binds with the thiourea N−H of **Cat**, consistent with the proposed structure of the **Cat**−**EI** complex (**Complex 3a**, Figure 3c). The slight change in the NMR spectra of the **Cat**−**EI** mixture indicates that the binding between **Cat** and **EI** is weaker than that between **Cat** and **Nu**, which is also supported by our theoretical calculation (vide supra).

Next, we examined the cases of the mixture of **Cat**, **Nu**, and **EI** via ^{1}H NMR spectroscopy at ambient temperature. When **EI** was added into the mixture of **Cat**−**Nu**, the N−H groups of thiourea were shifted 0.08 ppm to the downfield, and other protons in **Cat** remained almost unchanged (Figure S5). In contrast, upon the addition of **Nu** into the mixture of **Cat**−**EI**, almost all of the protons of **Cat** were shifted to downfield (Figure S6). These results further confirm that the binding of **Cat** with **Nu** is stronger than that with **EI** in the ternary **Cat**−**Nu**−**EI** complex.

It has been thought that the catalyst−substrate complexes could hardly be detected through the experimental methods.[8d] There has been no convincing experimental evidence to confirm the interaction between the catalyst and the substrates.[6a,c] As shown above, our ^{1}H NMR results successfully verified the formation of catalyst−substrate complexes via the hydrogen-bonding interaction. Also, our theoretical calculations predicted the stable structures of the catalyst−substrate complexes. Moreover, both the NMR measurement and the DFT calculation identified that **Cat** preferentially binds with **Nu** rather than with **EI** in the catalyst−substrate complexes.

Kinetic Studies. To obtain further information on the reaction mechanism, we conducted the kinetic studies via variable-temperature ^{1}H NMR experiments. The reaction was first carried out in $CDCl_3$ at 24 °C using the pseudo-first-order kinetics method. Plotting $-\ln([\mathbf{Nu}]/[\mathbf{Nu}^0])$ as a function of the reaction time gave a straight line (R^2 = 0.9988, Figure S7a), revealing that the reaction is first-order in **Nu**. In the same way, we determined that the reaction is also first-order in **EI** (R^2 = 0.9934, Figure S7b). By measuring the relative rate constant at different catalyst loadings (from 0.06 to 0.24 equiv), we found that the reaction is first-order in **Cat** as well (R^2 = 0.9957, Figure S7c). Therefore, the rate equation for this reaction can be described as: rate = k[**Cat**][**Nu**][**EI**]. Because only elementary reaction steps that occur before or at the rate-

dx.doi.org/10.1021/jo302133n | J. Org. Chem. 2012, 77, 9813−9825

determining step can be detected during a conventional kinetic study, these three species (**Cat**, **Nu**, and **EI**) must react before or at the rate-determining step. Because only two species (**Cat** and **Nu**, without **EI**) are involved in the process of **Cat** protonation (vide supra), we can experimentally rule out the protonation of **Cat** as the rate-determining step. Accordingly, the subsequent C−C bond formation or the recovery of **Cat** could be the rate-determining step for this reaction. This remark is further supported by our theoretical calculations (vide infra).

To determine the activation energy E_a, the rate constants k at T = 24, 30, 40, 50, and 60 °C were measured, respectively (see the Supporting Information for details). According to the logarithm form of Arrhenius equation, $\ln k = \ln A - E_a/RT$, plotting in $\ln k$ versus $1/T$ gave a straight line (R^2 = 0.9896, Figure 5). After the unit conversion, the experimental activation energy E_a was determined as 10.2 kcal/mol.

The kinetic studies have supplied important information on the rate equation and the experimental activation energy E_a, which will be compared to those derived from our theoretical calculations. To offer a complete picture on the detailed mechanism, such as the activation mode, the rate-determining step, and the origins for high enantio- and diastereoselectivity, we performed the DFT calculations on this reaction as follows.

Theoretical Results on the Main Product (5*R*, 6*S*). For the catalytic systems involving thiourea−tertiary amine organocatalysis, it has well been accepted that the catalyst activates both nucleophiles and electrophiles through hydrogen bonds. On the basis of this dual activation concept, two distinct activation mechanisms have been proposed by Takemoto[6a,9] and Pápai,[8d] respectively. In our catalytic system, according to Takemoto's proposal, **EI** should be activated by the thiourea N−H groups (both N−H_A and N−H_B), while **Nu** is activated by the N−H of the protonated amine (Scheme 3, Pathway A). On the contrary, according to Pápai's proposal, **Nu** should be activated by the thiourea N−H groups (both N−H_A and N−H_B), while **EI** is activated by the N−H of the protonated amine (Scheme 3, Pathway B).

We first applied the DFT calculations to explore these two possible pathways for the formation of the main product (5*R*, 6*S*). We found that Pathway B is theoretically possible. On the contrary, the initial ternary complexes or transition states hypothesized for Pathway A are unstable, and they were easily optimized to a new dual activation mode (Pathway C). In Pathway C (Scheme 3), one N−H group of thiourea (N−H_A) and the N−H of the protonated amine simultaneously activate **Nu**, while the other N−H group (N−H_B) activates **EI**. Accordingly, we present in this section the corresponding results for the formation of the main product (5*R*, 6*S*) via Pathway B and Pathway C, respectively. We found that the main product (5*R*, 6*S*) is produced predominantly via Pathway C instead of Pathway B.

As shown in Scheme 4, for Pathway B, we started from the most stable binary **Cat**−**Nu** complex (**Complex 2c**), in which the N−H of the protonated amine in **Cat** further interacts with **EI** via a hydrogen bond (length of 1.90 Å) to form a ternary complex $\mathbf{R}_{RS}\mathbf{B}$. The incoming of **EI** disturbs the hydrogen bond between **Nu** and the protonated amine, which makes **Nu** slightly move toward the thiourea N−H groups. The net result is that the interaction between **Cat** and **Nu** is weakened and the binding process is unfavorable, with a positive binding energy of 4.5 kcal/mol.

Scheme 4. Pathway B for the Formation of the Main Product (5*R*, 6*S*)

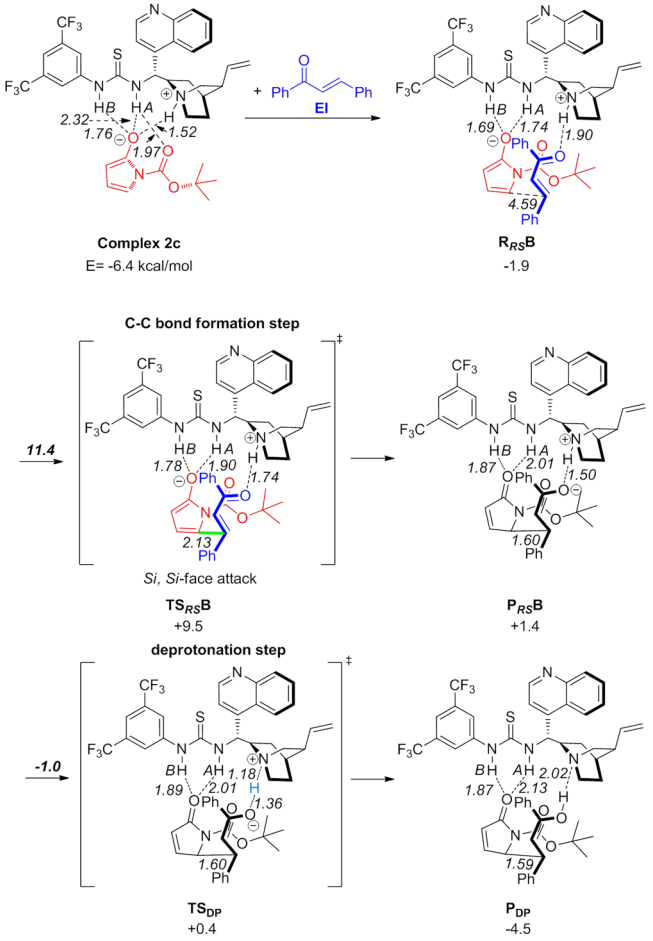

Moreover, the formed hydrogen bonds between the two substrates and **Cat** enhance not only the nucleophilicity of **Nu**, but also the electrophilicity of **EI**. The nucleophilic prochiral carbon of **Nu** and the electrophilic prochiral carbon of **EI** are spatially adjacent ($R_{C\cdots C}$ = 4.59 Å). Once the dual activation is accomplished, the C−C bond formation between the *Si* face of **Nu** and the *Si* face of **EI** subsequently takes place via a transition state $\mathbf{TS}_{RS}\mathbf{B}$, with an energy barrier of 11.4 kcal/mol. The transition state $\mathbf{TS}_{RS}\mathbf{B}$ is stabilized by the hydrogen-bonding interactions between **Cat** and the two substrates, and by the additional weak C−H···O interaction (length of 2.24 Å) between one C−H of the quinoline ring and the carbonyl oxygen of **EI** (Figure 6a). In this process, because of the negative charge transfer from **Nu** to **EI** and the charge delocalization, the hydrogen-bonding interaction between **Cat** and **EI** becomes stronger (with the length from 1.90 to 1.74, then to 1.50 Å, Scheme 4), accompanied by the weakening of the interaction between **Cat** and **Nu**.

The last stage of the catalytic cycle is the formation of product and the recovery of **Cat**, in which the preliminary adduct formed through the C−C bond formation first accepts a proton from the protonated **Cat** and dissociates from **Cat**, followed by the keto−enol tautomerization to afford the final product. In Pathway B, the negative energy barrier (−1.0 kcal/mol, Scheme 4) indicates that this step is a barrierless process, and therefore $\mathbf{P}_{RS}\mathbf{B}$ can very easily deprotonate the protonated amine of **Cat**. Because the energy barrier of this step is much

dx.doi.org/10.1021/jo302133n | J. Org. Chem. 2012, 77, 9813−9825

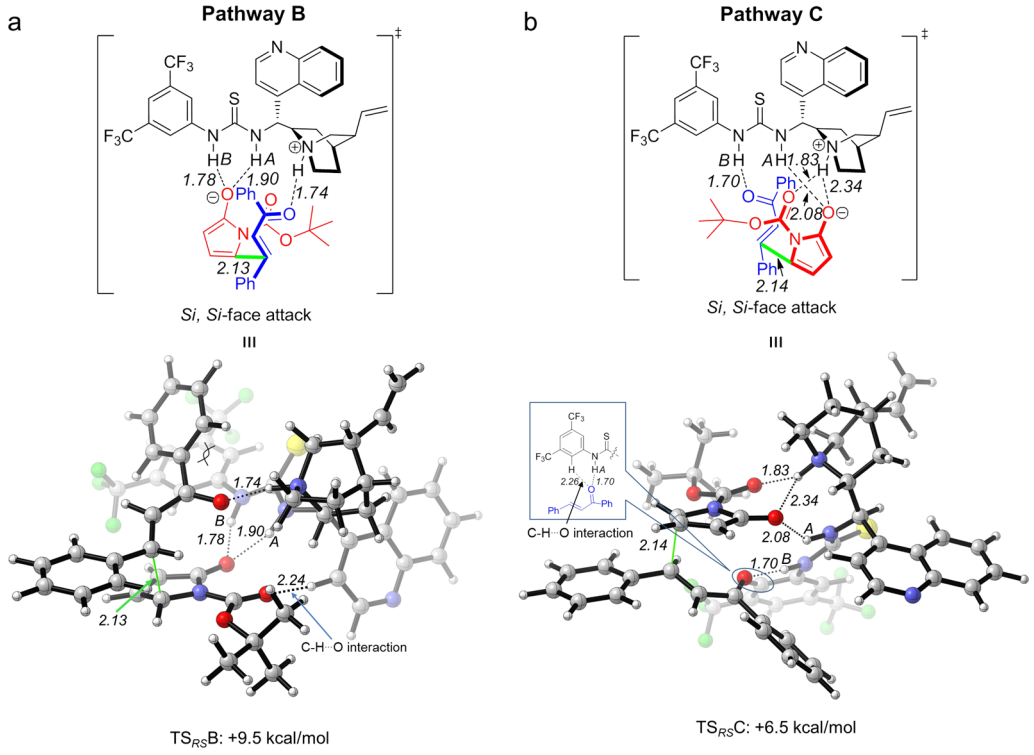

Figure 6. Transition state structures for the C−C bond formation in Pathway B (a, **TS$_{RS}$B**) and in Pathway C (b, **TS$_{RS}$C**), through which the main product (5*R*, 6*S*) is possibly formed.

lower than that of the C−C bond formation (11.4 kcal/mol), it can be concluded that the recovery of **Cat** by deprotonation is not the rate-determining step in Pathway B, and thus does not affect the stereoselectivity of the reaction products. Moreover, the enol form of the Michael adduct is readily tautomerized to its keto form.[28] Therefore, further investigation on this stage is not necessary.

In Pathway C (Scheme 5), the ternary complex **R$_{RS}$C** is formed from the binary **Complex 2a**[29] and **EI** via hydrogen-bond networks with a binding energy of −0.7 kcal/mol. In this ternary complex, **EI** forms a hydrogen bond (N−H$_B$···O, length of 1.91 Å) with the thiourea N−H$_B$, which makes **Nu** slightly move toward the N−H of the protonated amine. Therefore, the dual activation model of Pathway C is that **Nu** is simultaneously activated by the thiourea N−H$_A$ and the N−H of the protonated amine, while **EI** is activated by the thiourea N−H$_B$. In this case, although the two substrates simultaneously form the hydrogen bonds in the chiral pocket of **Cat**, the steric repulsion among **Cat**, **Nu**, and **EI** is very weak. As a result, these two substrates nearly remain at their best conformation without apparent torsions. In addition, the nucleophilic prochiral carbon of **Nu** and the electrophilic prochiral carbon of **EI** are spatially more adjacent ($R_{C\cdots C}$ = 3.87 Å) than in Pathway B ($R_{C\cdots C}$ = 4.59 Å). Accordingly, the C−C bond formation between the *Si* face of **Nu** and the *Si* face of **EI** subsequently takes place via a lower energy barrier (8.8 kcal/mol) in comparison with that in Pathway B (11.4 kcal/mol). In analogy to Pathway B, the C−C bond formation is accompanied by the negative charge transfer from **Nu** to **EI** and the charge delocalization, so the transition state for the C−C bond formation (**TS$_{RS}$C**) is stabilized by the weakened **Cat**−**Nu** interaction and the strengthened **Cat**−**EI** interaction. The additional C−H···O interaction between one C−H of 3,5-bis(trifluoromethyl) phenyl of **Cat** and the carbonyl oxygen of **EI** (Figure 6b) stabilizes **TS$_{RS}$C** as well.

Scheme 5. Pathway C for the Formation of the Main Product (5*R*, 6*S*)[29]

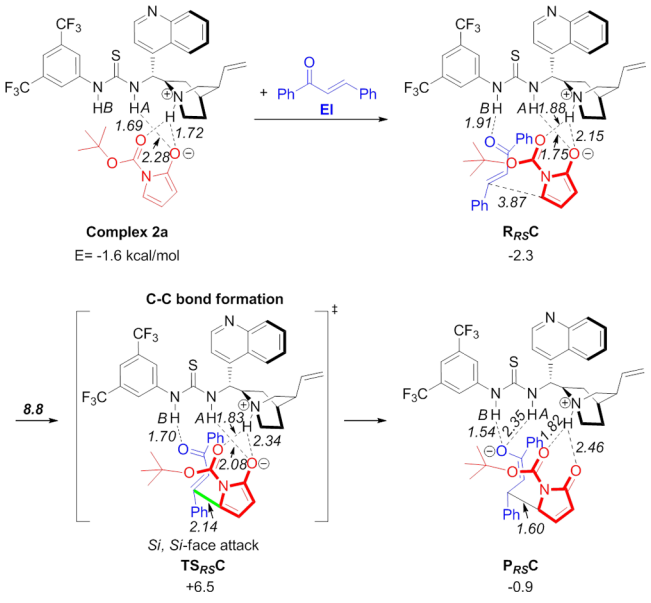

Comparison of Pathway B and Pathway C. For the purpose of convenient comparison, the calculated energy profiles of these two pathways for the main product (5*R*, 6*S*) are shown in Figure 7. All energies are relative to the total energy of the most stable conformer of **Cat**, **EI**, and the enolic **Nu**. The energy barriers for the protonation step are apparently lower than those of C−C bond formation in each pathway, indicating that the protonation step is not the rate-determining

dx.doi.org/10.1021/jo302133n | J. Org. Chem. 2012, 77, 9813−9825

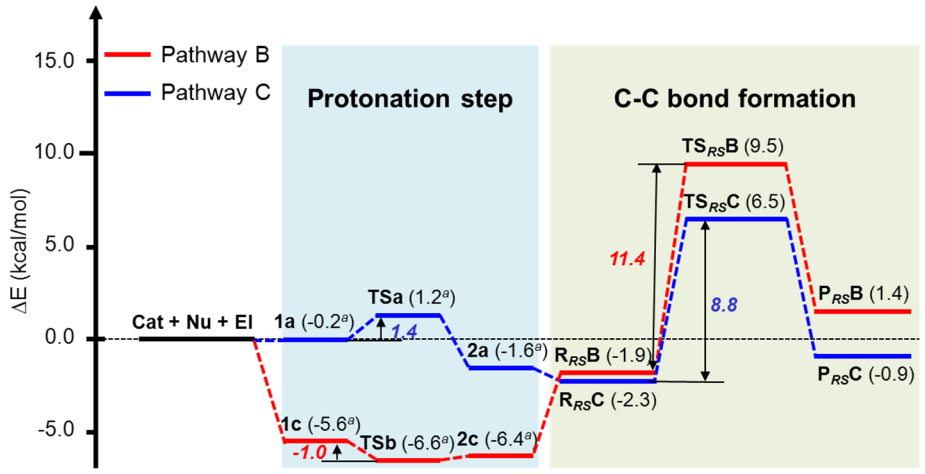

Figure 7. Energy profiles for the formation of the main product (5*R*, 6*S*) via Pathway B (red) and Pathway C (blue). [a]The energy of **EI** was also included for convenient comparison.

step. This result is well consistent with those obtained from kinetic studies (vide supra). Furthermore, as previously discussed, the last elementary step (**Cat** deprotonation) could be easily proceeded, and therefore is not the rate-determining step either. Accordingly, the C−C bond formation should be the rate-determining step for this reaction, which is consistent with the rate equation (rate = k[**Cat**][**Nu**][**EI**]) established in the kinetic studies.

Moreover, because all steps prior to the C−C bond formation are kinetically feasible and thermodynamically reversible, all of the binary and ternary catalyst−substrate complexes are in thermodynamic equilibria. Therefore, adjustment of the preferential pathway for the main product (5*R*, 6*S*) depends only on the comparison of the two transition states, $\mathbf{TS}_{RS}$**C** and $\mathbf{TS}_{RS}$**B**, for the C−C bond formation. Because the negative charge transfer from **Nu** to **EI** is followed by the charge delocalization, the hydrogen bonds between **Cat** and two substrates (especially **EI**) are important to stabilize these transition states. As can be seen from Figure 6, more hydrogen bonds exist between **Cat** and the two substrates in $\mathbf{TS}_{RS}$**C** than in $\mathbf{TS}_{RS}$**B**, and the length of the hydrogen bond between **Cat** and **EI** is shorter in $\mathbf{TS}_{RS}$**C**. Therefore, **Cat** can better stabilize $\mathbf{TS}_{RS}$**C** than $\mathbf{TS}_{RS}$**B**. Furthermore, in $\mathbf{TS}_{RS}$**B**, the steric repulsion among one phenyl group of **EI**, the 3,5-bis(trifluoromethyl) phenyl group, and the thiourea of **Cat** is so notable that the phenyl group of **EI** was significantly distorted from its best conformation. These effects make the energy of $\mathbf{TS}_{RS}$**B** 3.0 kcal/mol higher than that of $\mathbf{TS}_{RS}$**C** (Figure 7). Accordingly, the main product (5*R*, 6*S*) should be produced predominantly via Pathway C instead of Pathway B, and the ratio of the reaction rates along Pathway C and Pathway B is calculated as 109:1.

The calculated energy barrier for the rate-determining step in Pathway C is 8.8 kcal/mol, which represents a reasonable barrier height for the C−C bond formation step, if compared to the theoretical results for other organocatalytic C−C coupling reactions.[8d,p,30] In view of the fact that the DFT calculation would systematically underestimate the reaction barrier heights,[31] it is in good agreement between our theoretical (8.8 kcal/mol) and experimental (10.2 kcal/mol) results on the activation energy E_a.

Evidence from the Enantio- and Diastereoselectivity. To further validate the new dual activation mechanism, we conducted the DFT calculations on the theoretical values of enantio- and diastereoselectivity. We found that the calculated values based on Pathway C are well consistent with the experimental data. Because the C−C bond formation is the rate-determining step and the main product (5*R*, 6*S*) is produced predominantly via the Pathway C, we present herein the optimized structures and relative energies of the transition states (Figure 8) for the formation of the other three byproducts, that is, (5*S*, 6*R*), (5*S*, 6*S*), and (5*R*, 6*R*) along Pathway C.[32] The optimized structures and relative energies of other transition states along all pathways for these byproducts are included in the Supporting Information.

The byproduct (5*S*, 6*R*) is the enantiomer of the main product (5*R*, 6*S*). Therefore, the reaction enantioselectivity should be controlled by the relative energies of the transition states for the C−C bond formation (i.e., $\mathbf{TS}_{RS}$**C** and $\mathbf{TS}_{SR}$**C**). Because $\mathbf{TS}_{RS}$**C** is 3.9 kcal/mol more stable than $\mathbf{TS}_{SR}$**C**, the level of enantioselectivity is predicted as 100% ee, which is in excellent agreement with our experimental result (98% ee). In the transition state of the main product (5*R*, 6*S*) ($\mathbf{TS}_{RS}$**C**, Figure 6b), the hydrogen bonds between **Cat** and the two substrates, especially between the thiourea N−H_B and **EI**, are shorter than that for byproduct (5*S*, 6*R*) ($\mathbf{TS}_{SR}$**C**, Figure 8a). Because the negative charge would be transferred from **Nu** to **EI**, the shorter hydrogen bond between the thiourea N−H_B and **EI** is more favorable for stabilizing the corresponding transition state. This implies that the enantioselectivity control in cinchona alkaloid thiourea organocatalysis is affected, to a certain extent, by the acidity of the thiourea N−H_B, which could be tuned by changing the electron-deficient nature of the adjacent aromatic ring. Electron-donating substituents in the aromatic ring would lower the enantioselectivity, while electron-withdrawing substituents enhance it. This remark has found strong support from the previous experimental work.[6a,g,9] In addition, $\mathbf{TS}_{SR}$**C** exhibits serious steric repulsion between one phenyl group of **EI** and the bulky quinuclidine moiety of **Cat**. On the contrary, in $\mathbf{TS}_{RS}$**C**, the steric repulsion among **Cat**, **Nu**, and **EI** is very weak. Accordingly, the high enantioselectivity is caused by the stronger hydrogen-bonding interaction between the thiourea N−H_B and **EI** in the formation process of the main product (5*R*, 6*S*), and by the serious steric repulsion between **EI** and **Cat** in the formation process of the enantiomer (5*S*, 6*R*).

dx.doi.org/10.1021/jo302133n | J. Org. Chem. 2012, 77, 9813−9825

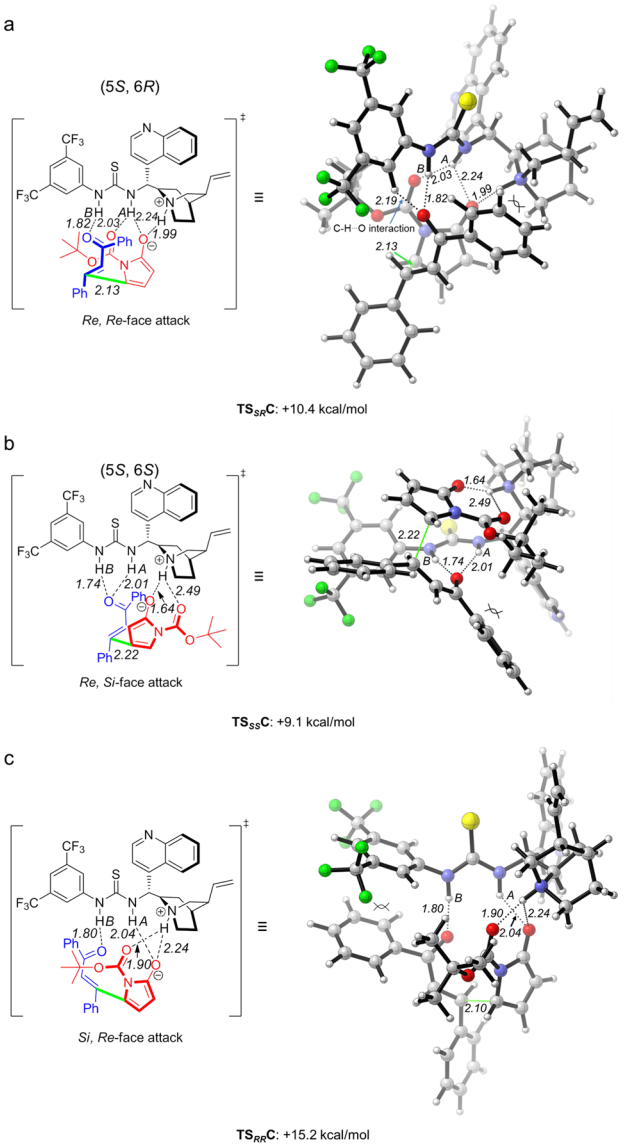

Figure 8. Optimized structures and relative energies of the transition states, which afford the enantiomer (5*S*, 6*R*) (a), one diastereoisomer (5*S*, 6*S*) (b), and the other diastereoisomer (5*R*, 6*R*) (c) via Pathway C.

On the basis of the relative energies of the transition states for the four stereoisomeric products along Pathway C, the diastereoselectivity could be predicted as 60:1, which agrees excellently with our experimental[13] result (>30:1 dr) as well. Furthermore, the transition state of one diastereoisomer (5*S*, 6*S*) (**TS$_{SS}$C**, 9.1 kcal/mol) is much more stable than that of the other diastereoisomer (5*R*, 6*R*) (**TS$_{RR}$C**, 15.2 kcal/mol), and therefore the primary diastereoisomer is the byproduct (5*S*, 6*S*). Because of the high enantioselectivity (experimental 98% and calculated 100%), the reaction diastereoselectivity predominantly depends on the product ratio of the main product (5*R*, 6*S*) and the byproduct (5*S*, 6*S*). Thus, this diastereoselectivity value is determined by the relative energies of their transition states, that is, **TS$_{RS}$C** (6.5 kcal/mol) and **TS$_{SS}$C** (9.1 kcal/mol).

Comparing the structures of **TS$_{RS}$C** and **TS$_{SS}$C** (Figure 6b and Figure 8b), we found that serious steric repulsion exists between one phenyl group of **EI** and the *tert*-butyl group of **Nu** in **TS$_{SS}$C**, but is absent in **TS$_{RS}$C**. In addition, in **TS$_{RS}$C**, except the normal hydrogen bonds, weak C−H···O interaction between one C−H of 3,5-bis(trifluoromethyl) phenyl group of **Cat** and the carbonyl oxygen of **EI** also stabilizes **TS$_{RS}$C**. This effect is absent in **TS$_{SS}$C** as well. All of these effects make **TS$_{RS}$C** 2.6 kcal/mol more stable than **TS$_{SS}$C**. Therefore, the origin of the high diastereoselectivity is mainly due to the existence of serious steric repulsion between one phenyl group of **EI** and the *tert*-butyl group of **Nu** when the primary diastereoisomer (5*S*, 6*S*) is formed. Additional weak C−H···O interaction between one C−H of 3,5-bis(trifluoromethyl) phenyl group of **Cat** and the carbonyl oxygen of **EI** in the formation process of the main product (5*R*, 6*S*) also contributes to the high diastereoselectivity.

The excellent match between the calculated (100% ee and 60:1 dr, respectively) and the experimental (98% ee and >30:1 dr, respectively) data for the enantio- and diastereoselectivity further evidences the validity of Pathway C. On the other hand, on the basis of the relative energies of the transition states along Pathway B (see Supporting Information for details), the enantio- and diastereoselectivity are calculated as 76% ee and 3:1 dr, respectively. The poor consistency between the calculated and the experimental values also implies that this reaction is unlikely to occur via Pathway B.

Scope for the Activation Mechanism along Pathway C. As addressed above, the investigated reaction (Scheme 1) follows a new dual activation mechanism (Pathway C, Scheme 3). To further verify the generality of this new mechanism, we next examined the possible activation process for the Michael addition of nitromethane to chalcone[21b] (Scheme 6) catalyzed by a bifunctional cinchona alkaloid thiourea organocatalyst (**Catalyst I** in Figure 1b). This reaction was experimentally carried out in toluene with 94% yield and 96% ee.[21b] The calculation details are the same as those for the above reaction, except that the solvent used (toluene) is consistent with the original experiment.

We explored the three possible activation mechanisms (Pathway A, B, and C) for this reaction. In the structure of the starting ternary complex in Pathway B, nitromethane is simultaneously activated by the two functional groups of **Catalyst I**, while chalcone is not activated at all. Because this activation model does not fit with the dual activation concept, we paid our attention to Pathway A and Pathway C only (Scheme 6). We found that the transition state of Pathway C (**TSC**, 11.9 kcal/mol) is 1.1 kcal/mol more stable than that of Pathway A (**TSA**, 13.0 kcal/mol). Accordingly, this reaction occurs preferentially with the Pathway C as well, and the ratio of the reaction rates along Pathway C and Pathway A is calculated as 6:1.[33] Because **Catalyst I** owns the opposite configuration of both C8 and C9 in comparison with **Cat**, the stereochemistry of C8 and C9 has no effect on the dual activation model of cinchona alkaloid thiourea organocatalysis. Moreover, when the electrophile chalcone is kept unchanged, even though the bulky nucleophile (*α*,*β*-unsaturated *γ*-butyrolactam, Scheme 1) is replaced with a small one (nitromethane, Scheme 6), the dual activation model of cinchona alkaloid thiourea organocatalysis still follows Pathway C. This result implies that Pathway C could be applicable at least to diverse cinchona alkaloid thiourea organocatalysts with different nucleophiles.

As Takemoto's (Pathway A) and Pápai's (Pathway B) proposals, the newly discovered mechanism (Pathway C) is still consistent with the dual activation concept, because both

dx.doi.org/10.1021/jo302133n | J. Org. Chem. 2012, 77, 9813−9825

Scheme 6. Michael Addition of Nitromethane to Chalcone Catalyzed by Catalyst I[a]

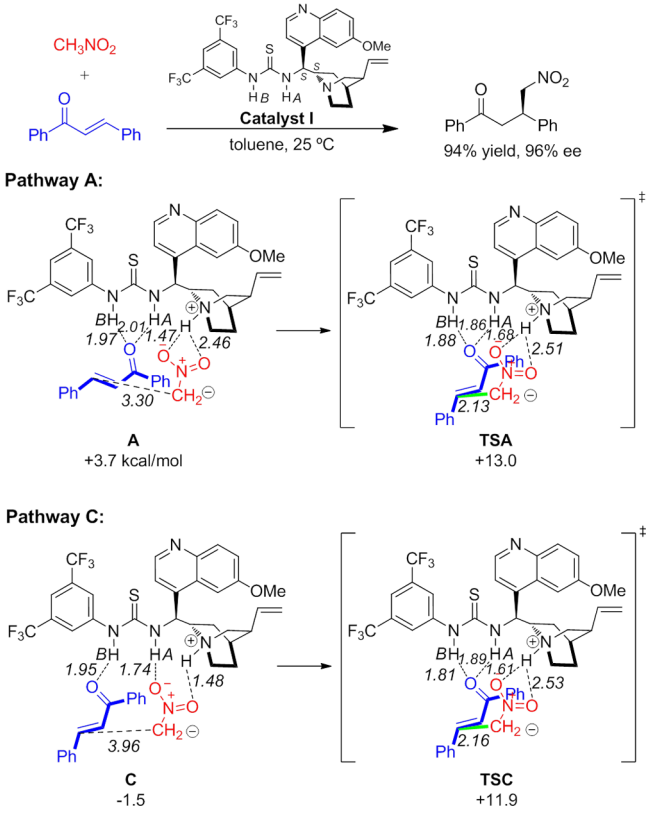

[a]Energies are relative to the total energies of the catalyst and two substrates.

substrates are simultaneously activated by **Cat** within a ternary complex. In either Pathway A or Pathway B, however, it is assumed that the two thiourea N−H groups (N−H_A and N−H_B) play the same role at the same time in activating one substrate only (nucleophile or electrophile). In fact, the two electron-withdrawing $-CF_3$ substituents in the phenyl group of **Cat** increase the acidity of thiourea N−H_B,[34] which makes thiourea N−H_B more acidic than N−H_A. At −80 °C, the ^{1}H NMR spectra of cinchona alkaloid thiourea organocatalysts in CD_2Cl_2 showed that the chemical shifts of thiourea N−H_A and N−H_B are 7.6−7.8 and 11.8−12.1 ppm, respectively.[35] Moreover, the N−H_A is spatially adjacent to the quinuclidine amine. Therefore, the thiourea N−H_A and N−H_B could essentially play different roles in activating the (different) substrates. Our results presented in this contribution indicate that the thiourea N−H_A and the N−H of the protonated amine simultaneously activate the nucleophile, while the thiourea N−H_B activates the electrophile (Pathway C, Scheme 3).

This new activation model may provide further insight into the bifunctional reactivity of thiourea−tertiary amine organocatalysts and their analogues. For example, Rawal and his coworkers[36] have recently developed the chiral squaramide derivatives (Figure 9) as an excellent type of hydrogen-bonding organocatalysts. These chiral squaramides have found diverse applications[37] in many organocatalytic reactions with excellent efficiency. In these squaramide organocatalysts, the distance between the two N−H protons is estimated as ∼2.7 Å, which is 0.6 Å further apart than that found in thioureas (∼2.1 Å). The activation mechanisms involved in the squaramide-based

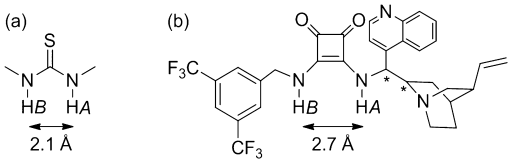

Figure 9. Chiral squaramide-based bifunctional catalysts (b). The distance between the two N−H protons is 0.6 Å further apart than that in thiourea organocatalysts (a).

bifunctional catalysis may also preferentially follow Pathway C. Moreover, the thiourea moiety is an outstanding functional group for mimicking the hydrogen-bonding sites of the enzyme catalysts.[38] The concept that two thiourea N−H groups (N−H_A and N−H_B) play different roles in activating the (different) substrates may help in the rational design of biomimetic organocatalytic systems as well.

SUMMARY AND CONCLUSION

In this Article, we have conducted both experimental and computational investigations on the direct asymmetric vinylogous Michael reaction of α,β-unsaturated γ-butyrolactam (**Nu**) and chalcone (**EI**) catalyzed by the bifunctional cinchona alkaloid thiourea organocatalyst (**Cat**). The main conclusions drawn from our investigations are summarized as follows:

(1) The calculated **Cat** structure indicates that the thiourea N−H groups and the quinuclidine amine moiety orient to the same direction in the chiral scaffold. These two active sites in the particular spatial arrangement, together with the quinoline ring and the quinuclidine moiety provide an active chiral pocket, which is ideal for the dual activation of both **Nu** and **EI**. As a result, the perfect control of the reaction stereoselectivity could be achieved.

(2) Via the DFT calculations, we found the most stable structures for the catalyst−substrate complexes. Via the ^{1}H NMR measurements, we verified the hydrogen-bonding interaction between the catalyst and the substrates. Both experimental and theoretical results revealed that the interaction of **Cat** with **Nu** is stronger than that with **EI** in the catalyst−substrate complexes.

(3) The kinetic studies indicated that this reaction is all first-order in **Nu**, **EI**, and **Cat**, and thus ruled out the protonation of **Cat** as the rate-determining step. The experimental activation energy E_a was measured to be 10.2 kcal/mol. Moreover, the DFT calculations revealed that the rate-determining step is the C−C bond formation, which controls the reaction stereoselectivity.

(4) The enantio- and diastereoselectivity derived theoretically are in excellent agreement with the experimental results. The high enantioselectivity is caused by the stronger hydrogen-bonding interaction between the thiourea N−H_B and **EI** in the formation process of the main product (5*R*, 6*S*), together with the serious steric repulsion between the phenyl of **EI** and the bulky quinuclidine moiety of **Cat** in the formation process of the enantiomer (5*S*, 6*R*). The origin of high diastereoselectivity comes from the existence of serious steric repulsion between the phenyl of **EI** with the *tert*-buty of **Nu** during the formation of the primary diastereoisomer (5*S*, 6*S*), together with the additional weak C−H···O

dx.doi.org/10.1021/jo302133n | J. Org. Chem. 2012, 77, 9813−9825

stabilization effect in the formation process of the main product (5*R*, 6*S*).

(5) Our DFT calculations revealed a new dual activation mechanism (Pathway C), in which one N−H_A of the thiourea moiety and the N−H of the protonated amine in **Cat** simultaneously activate **Nu**, while the other N−H_B of the thiourea moiety activates **EI**. The validity of Pathway C was further evidenced by the calculated enantioselectivity (100% ee) and diastereoselectivity (60:1 dr) along Pathway C, which are in excellent match with the experimental data (98% ee and >30:1 dr, respectively). Further studies on other catalytic system indicate that Pathway C can be applicable to the cinchona alkaloid thiourea organocatalysis with different nucleophiles. This information may offer further insight into the bifunctional nature of the thiourea−tertiary amine organocatalysts and extend the understanding of biomimetic bifunctional organocatalysis.

EXPERIMENTAL SECTION

The catalyst (**Cat**) was synthesized according to the published procedures.[21]

NMR Characterization of the Catalyst (Cat). Amorphous solid. ^{1}H NMR (400 MHz, $CDCl_3$, δ_{TMS} = 0 ppm): δ 9.71 (br, N−H), 8.71 (br, 1H, H2′), 8.36 (br, 1H, H5′), 8.09 (d, J = 7.7 Hz, 1H, H8′), 7.90 (br, 2H, 2H2″), 7.71 (m, 1H, H7′), 7.65 (br, 1H, H4″), 7.62 (m, 1H, H6′), 7.28 (unresolved, partially overlapped by $CDCl_3$, 1H, H3′), 5.99 (unresolved, partially overlapping signals, 1H, H9), 5.85 (unresolved, partially overlapping signals, 1H, *CH*=CH_2), 5.20 (m, 2H, CH=*C*H_2), 3.25 (br, 1H, H8), 3.10 (m, 1H, H2-*exo*), 2.94 (m, 2H, H6α and H2-*endo*), 2.79 (br, 1H, H6β), 2.35 (m, 1H, H3), 1.66 (s, 1H, H4), 1.57 (unresolved, partially overlapping signals, 1H, H5α), 1.48 (unresolved, partially overlapping signals, 1H, H5β), 1.26 (m, 1H, H7β), 0.90 (m, 1H, H7α) ppm. ^{13}C NMR (100 MHz, $CDCl_3$, δ_{TMS} = 0 ppm): δ 180.9 (C=S), 150.0 (C2′), 148.5 (C4′), 146.0 (C8a′), 140.2 (C1″), 138.9 (*C*H=CH_2), 132.4 (q, $^2J_{CF}$ = 33.3 Hz, C3″), 130.3 (C8′), 129.6 (C7′), 127.2 (C6′), 123.0 (q, $^1J_{CF}$ = 273.0 Hz, CF_3), 123.5 (br signal, C2″ and C5′), 119.3 (br signal, C3′), 118.6 (C4″), 115.8 (CH=*C*H_2), 61.5 (C8), 55.1 (C9), 48.5 (C6), 46.9 (C2), 38.5 (C3), 27.1 (C4), 25.6 (C5), 24.8 (C7) ppm. The weak signal of quaternary carbon C4a′ is likely overlapped by other signals of **Cat**.

ASSOCIATED CONTENT

Supporting Information

NMR characterization of the catalyst (**Cat**), ^{1}H NMR investigation on the hydrogen-bonding interaction, detailed results of kinetic studies, complete ref 17, conformational analysis on **Cat** and chalcone (**EI**), structures and binding energies of the binary **Cat**−**EI** complexes, optimized structures and relative energies of the transition states for the other three byproducts, and the Cartesian coordinates and total electronic energies of all reported structures. This material is available free of charge via the Internet at http://pubs.acs.org.

AUTHOR INFORMATION

Corresponding Author

*E-mail: wang_wei@lzu.edu.cn.

Notes

The authors declare no competing financial interest.

ACKNOWLEDGMENTS

We are grateful for financial support from the National Natural Science Foundation of China (nos. 20933009 and 20972064), the Key Grant Project of Chinese Ministry of Education (no. 309028), and the 111 Project. We also acknowledge the computing resources and time on the Supercomputing Center of Cold and Arid Region Environment and Engineering Research Institute of Chinese Academy of Sciences.

REFERENCES

(1) For some recent books, see: (a) Berkessel, A.; Gröger, H. *Asymmetric Organocatalysis*; Wiley Online Library, 2005. (b) List, B. *Asymmetric Organocatalysis*; Springer: New York, 2010. (c) Pellissier, H. *Recent Developments in Asymmetric Organocatalysis*; RSC Publishing: Cambridge, 2010.

(2) (a) MacMillan, D. W. C. *Nature* **2008**, *455*, 304. For the original reports on new activation modes, see, for example: (b) Miller, S. J.; Copeland, G. T.; Papaioannou, N.; Horstmann, T. E.; Ruel, E. M. *J. Am. Chem. Soc.* **1998**, *120*, 1629. (c) Sigman, M. S.; Jacobsen, E. N. *J. Am. Chem. Soc.* **1998**, *120*, 4901. (d) Corey, E. J.; Grogan, M. J. *Org. Lett.* **1999**, *1*, 157. (e) Ahrendt, K. A.; Borths, C. J.; MacMillan, D. W. C. *J. Am. Chem. Soc.* **2000**, *122*, 4243. (f) King, H. D.; Meng, Z.; Denhart, D.; Mattson, R.; Kimura, R.; Wu, D.; Gao, Q.; Macor, J. E. *Org. Lett.* **2005**, *7*, 3437. (g) Jang, H.-Y.; Hong, J.-B.; MacMillan, D. W. C. *J. Am. Chem. Soc.* **2007**, *129*, 7004. (h) Reisman, S. E.; Doyle, A. G.; Jacobsen, E. N. *J. Am. Chem. Soc.* **2008**, *130*, 7198.

(3) For the selected reviews on the activation modes, see: (a) Erkkilä, A.; Majander, I.; Pihko, P. M. *Chem. Rev.* **2007**, *107*, 5416. (b) Mukherjee, S.; Yang, J. W.; Hoffmann, S.; List, B. *Chem. Rev.* **2007**, *107*, 5471. (c) Enders, D.; Niemeier, O.; Henseler, A. *Chem. Rev.* **2007**, *107*, 5606. (d) Doyle, A. G.; Jacobsen, E. N. *Chem. Rev.* **2007**, *107*, 5713. (e) Luo, S.; Zhang, L.; Cheng, J.-P. *Chem.-Asian J.* **2009**, *4*, 1184. (f) Shao, Z.; Zhang, H. *Chem. Soc. Rev.* **2009**, *38*, 2745. (g) Cheong, P. H.-Y.; Legault, C. Y.; Um, J. M.; Çelebi-Ölçüm, N.; Houk, K. N. *Chem. Rev.* **2011**, *111*, 5042.

(4) For the selected reviews on the bifunctional catalysis, see: (a) Takemoto, Y. *Org. Biomol. Chem.* **2005**, *3*, 4299. (b) Marcelli, T.; van Maarseveen, J. H.; Hiemstra, H. *Angew. Chem., Int. Ed.* **2006**, *45*, 7496. (c) Miyabe, H.; Takemoto, Y. *B. Chem. Soc. Jpn.* **2008**, *81*, 785. (d) Connon, S. J. *Chem. Commun.* **2008**, 2499. (e) Zhang, Z. G.; Schreiner, P. R. *Chem. Soc. Rev.* **2009**, *38*, 1187. (f) Leow, D.; Tan, C.-H. *Chem.-Asian J.* **2009**, *4*, 488. (g) Takemoto, Y. *Chem. Pharm. Bull.* **2010**, *58*, 593. (h) Sohtome, Y.; Nagasawa, K. *Synlett* **2010**, *2010*, 1. (i) Mansilla, J.; Saa, J. M. *Molecules* **2010**, *15*, 709. (j) Siau, W.-Y.; Wang, J. *Catal. Sci. Technol.* **2011**, *1*, 1298. (k) Briere, J.-F.; Oudeyer, S.; Dalla, V.; Levacher, V. *Chem. Soc. Rev.* **2012**, *41*, 1696.

(5) For the latest examples, see, for example: (a) Bai, J.-F.; Wang, L.-L.; Peng, L.; Guo, Y.-L.; Jia, L.-N.; Tian, F.; He, G.-Y.; Xu, X.-Y.; Wang, L.-X. *J. Org. Chem.* **2012**, *77*, 2947. (b) Sun, Z.-W.; Peng, F.-Z.; Li, Z.-Q.; Zou, L.-W.; Zhang, S.-X.; Li, X.; Shao, Z.-H. *J. Org. Chem.* **2012**, *77*, 4103. (c) Asano, K.; Matsubara, S. *Org. Lett.* **2012**, *14*, 1620. (d) Zhong, F.; Luo, J.; Chen, G.-Y.; Dou, X.; Lu, Y. *J. Am. Chem. Soc.* **2012**, *134*, 10222. (e) Rajkumar, S.; Shankland, K.; Brown, G. D.; Cobb, A. J. A. *Chem. Sci.* **2012**, *3*, 584. (f) Huang, H.; Zhu, K.; Wu, W.; Jin, Z.; Ye, J. *Chem. Commun.* **2012**, *48*, 461.

(6) (a) Okino, T.; Hoashi, Y.; Furukawa, T.; Xu, X.; Takemoto, Y. *J. Am. Chem. Soc.* **2005**, *127*, 119. (b) Hoashi, Y.; Okino, T.; Takemoto, Y. *Angew. Chem., Int. Ed.* **2005**, *44*, 4032. (c) Inokuma, T.; Hoashi, Y.; Takemoto, Y. *J. Am. Chem. Soc.* **2006**, *128*, 9413. (d) Zuend, S. J.; Jacobsen, E. N. *J. Am. Chem. Soc.* **2007**, *129*, 15872. (e) Zuend, S. J.; Jacobsen, E. N. *J. Am. Chem. Soc.* **2009**, *131*, 15358. (f) Kataja, A. O.; Koskinen, A. M. P. *Arkivoc* **2010**, 205. (g) Li, X.; Deng, H.; Zhang, B.; Li, J. Y.; Zhang, L.; Luo, S. Z.; Cheng, J. P. *Chem.-Eur. J.* **2010**, *16*, 450.

(7) Houk, K. N.; Cheong, P. H.-Y. *Nature* **2008**, *455*, 309.

(8) For the representative theoretical work on the bifunctional thiourea organocatalysis, see: (a) Zhu, Y.; Drueckhammer, D. G. *J. Org. Chem.* **2005**, *70*, 7755. (b) Yalalov, D. A.; Tsogoeva, S. B.; Schmatz, S. *Adv. Synth. Catal.* **2006**, *348*, 826. (c) Zhu, R.; Zhang, D.; Wu, J.; Liu, C. *Tetrahedron: Asymmetry* **2006**, *17*, 1611. (d) Hamza, A.; Schubert, G.; Soós, T.; Pápai, I. *J. Am. Chem. Soc.* **2006**, *128*, 13151. (e) Liu, T.-Y.; Li, R.; Chai, Q.; Long, J.; Li, B.-J.; Wu, Y.; Ding, L.-S.; Chen, Y.-C. *Chem.-Eur. J.* **2007**, *13*, 319. (f) Hammar, P.; Marcelli, T.;

Hiemstra, H.; Himo, F. *Adv. Synth. Catal.* **2007**, *349*, 2537. (g) Wei, S.; Yalalov, D. A.; Tsogoeva, S. B.; Schmatz, S. *Catal. Today* **2007**, *121*, 151. (h) Rokob, T. A.; Hamza, A.; Pápai, I. *Org. Lett.* **2007**, *9*, 4279. (i) Zhu, R.; Zhang, D.; Wu, J.; Liu, C. *Tetrahedron: Asymmetry* **2007**, *18*, 1655. (j) Zhang, D.; Wang, G.; Zhu, R. *Tetrahedron: Asymmetry* **2008**, *19*, 568. (k) Chen, D.; Lu, N.; Zhang, G.; Mi, S. *Tetrahedron: Asymmetry* **2009**, *20*, 1365. (l) Simon, L.; Goodman, J. M. *Org. Biomol. Chem.* **2009**, *7*, 483. (m) Wang, S.-X.; Chen, F.-E. *Adv. Synth. Catal.* **2009**, *351*, 547. (n) Xu, H.; Zuend, S. J.; Woll, M. G.; Tao, Y.; Jacobsen, E. N. *Science* **2010**, *327*, 986. (o) Tan, B.; Lu, Y. P.; Zeng, X. F.; Chua, P. J.; Zhong, G. F. *Org. Lett.* **2010**, *12*, 2682. (p) Manzano, R.; Andrés, J. M.; Álvarez, R.; Muruzábal, M. D.; de Lera, Á. R.; Pedrosa, R. *Chem.-Eur. J.* **2011**, *17*, 5931. (q) Li, X.; Xue, X.-S.; Liu, C.; Wang, B.; Tan, B.-X.; Jin, J.-L.; Zhang, Y.-Y.; Dong, N.; Cheng, J.-P. *Org. Biomol. Chem.* **2012**, *10*, 413.

(9) Okino, T.; Hoashi, Y.; Takemoto, Y. *J. Am. Chem. Soc.* **2003**, *125*, 12672.

(10) For the representative experimental work favoring Pathway A, see: (a) Wang, B.; Wu, F.; Wang, Y.; Liu, X.; Deng, L. *J. Am. Chem. Soc.* **2007**, *129*, 768. (b) Wang, F.; Liu, X.; Cui, X.; Xiong, Y.; Zhou, X.; Feng, X. *Chem.-Eur. J.* **2009**, *15*, 589. (c) Basle, O.; Raimondi, W.; Sanchez Duque, M. d. M.; Bonne, D.; Constantieux, T.; Rodriguez, J. *Org. Lett.* **2010**, *12*, 5246. (d) Rana, N. K.; Singh, V. K. *Org. Lett.* **2011**, *13*, 6520. (e) Alcaine, A.; Marques-Lopez, E.; Merino, P.; Tejero, T.; Herrera, R. P. *Org. Biomol. Chem.* **2011**, *9*, 2777. (f) Li, X.-J.; Peng, F.-Z.; Li, X.; Wu, W.-T.; Sun, Z.-W.; Li, Y.-M.; Zhang, S.-X.; Shao, Z.-H. *Chem.-Asian J.* **2011**, *6*, 220. (g) Zhao, M.-X.; Tang, W.-H.; Chen, M.-X.; Wei, D.-K.; Dai, T.-L.; Shi, M. *Eur. J. Org. Chem.* **2011**, 6078. (h) Zhang, T.; Cheng, L.; Hameed, S.; Liu, L.; Wang, D.; Chen, Y.-J. *Chem. Commun.* **2011**, *47*, 6644.

(11) For the representative experimental work favoring Pathway B, see: (a) Wang, X.-F.; Peng, L.; An, J.; Li, C.; Yang, Q.-Q.; Lu, L.-Q.; Gu, F.-L.; Xiao, W.-J. *Chem.-Eur. J.* **2011**, *17*, 6484. (b) Shao, Y.-D.; Tian, S.-K. *Chem. Commun.* **2012**, *48*, 4899. (c) Tan, B.; Zeng, X.; Leong, W. W. Y.; Shi, Z.; Barbas, C. F., III; Zhong, G. *Chem.-Eur. J.* **2012**, *18*, 63. (d) Dou, X.; Han, X.; Lu, Y. *Chem.-Eur. J.* **2012**, *18*, 85.

(12) Gridnev, I. D.; Watanabe, M.; Wang, H.; Ikariya, T. *J. Am. Chem. Soc.* **2010**, *132*, 16637.

(13) Zhang, Y.; Shao, Y.-L.; Xu, H.-S.; Wang, W. *J. Org. Chem.* **2011**, *76*, 1472.

(14) The change (ΔG) in the Gibbs free energy for the keto−enol tautomeric equilibrium is 8.8 kcal/mol, derived from the frequency analysis at B3LYP/6-31G(d,p) (CPCM, $CHCl_3$) level. Therefore, the keto−enol tautomeric equilibrium of **Nu** should shift toward the formation of ketone. Accordingly, the enolic **Nu** with higher activity is applied in the computational calculation. The same concept has previously been acknowledged in other work (see, for example: *J. Org. Chem.* **2004**, *69*, 6603).

(15) The solvents were found to have a dramatic influence on the reaction yields and the stereoselectivity. $CHCl_3$ and toluene were screened as the best reaction media in the original experiments; see ref 13.

(16) (a) Lee, C.; Yang, W.; Parr, R. G. *Phys. Rev. B* **1988**, *37*, 785. (b) Becke, A. D. *J. Chem. Phys.* **1993**, *98*, 5648. (c) Becke, A. D. *J. Chem. Phys.* **1993**, *98*, 1372.

(17) Frisch, M. J.; et al. *Gaussian 09*, revision A.01; Gaussian, Inc.: Wallingford, CT, 2009.

(18) (a) Barone, V.; Cossi, M. *J. Phys. Chem. A* **1998**, *102*, 1995. (b) Cossi, M.; Rega, N.; Scalmani, G.; Barone, V. *J. Comput. Chem.* **2003**, *24*, 669.

(19) (a) Fukui, K. *Acc. Chem. Res.* **1981**, *14*, 363. (b) Gonzalez, C.; Schlegel, H. B. *J. Chem. Phys.* **1989**, *90*, 2154. (c) Gonzalez, C.; Schlegel, H. B. *J. Phys. Chem.* **1990**, *94*, 5523.

(20) Legault, C. Y. *CYLview, 1.0b*; Université de Sherbrooke, 2009; http://www.cylview.org.

(21) (a) Li, B.-J.; Jiang, L.; Liu, M.; Chen, Y.-C.; Ding, L.-S.; Wu, Y. *Synlett* **2005**, *2005*, 603. (b) Vakulya, B.; Varga, S.; Csámpai, A.; Soós, T. *Org. Lett.* **2005**, *7*, 1967.

(22) For the details of conformational analysis including the other less stable conformations, see the Supporting Information.

(23) Oh, J.-S.; Lee, J.-W.; Ryu, T. H.; Lee, J. H.; Song, C. E. *Org. Biomol. Chem.* **2012**, *10*, 1052.

(24) For the selected examples, see: (a) Agmon, N. *J. Phys. Chem. B* **2007**, *111*, 7870. (b) Xia, Y.; Liang, Y.; Chen, Y.; Wang, M.; Jiao, L.; Huang, F.; Liu, S.; Li, Y.; Yu, Z.-X. *J. Am. Chem. Soc.* **2007**, *129*, 3470. (c) Climent, M. J.; Corma, A.; Domínguez, I.; Iborra, S.; Sabater, M. J.; Sastre, G. *J. Catal.* **2007**, *246*, 136.

(25) The values of Gibbs free energies are derived from the frequency analysis at the B3LYP/6-31G(d,p) (CPCM, $CHCl_3$) level.

(26) The formation of zwitterionic **Cat**−**Nu** complex is significantly affected by the solvents used in the NMR experiments. We could not identify the interaction between **Cat** and **Nu** in $CDCl_3$, which is masked by the stronger interaction between $CDCl_3$ and the carbonyl oxygen of **Nu** through C−H···O hydrogen bonds (see: *New J. Chem.* **1998**, *22*, 1099; *Org. Lett.* **2000**, *2*, 3321; *J. Am. Chem. Soc.* **2002**, *124*, 9662; *J. Org. Chem.* **2003**, *68*, 8662). Without destroying the initial hydrogen bonds, the use of C_6D_6 as the solvent can further stabilize the zwitterionic **Cat**−**Nu** complex by the cation−π interaction between the protonated **Cat** and the benzene ring (see: *Proc. Natl. Acad. Sci. U.S.A.* **1998**, *95*, 12088). Accordingly, we selected C_6D_6 as the solvent to visualize the interaction between **Cat** and **Nu**.

(27) The chemical shifts for the two protons in the thiourea N−H groups should be varied more apparently than other protons when **Cat** interacts with **Nu**. Being too active at ambient temperature (see ref 35), the thiourea N−H_B only shows a broad weak signal in C_6D_6 at 24 °C, while the thiourea N−H_A could not be unambiguously detected due to the overlapping by other protons.

(28) Guthrie, J. P.; Cullimore, P. A. *Can. J. Chem.* **1979**, *57*, 240.

(29) Upon the theoretical calculations on the main product (5*R*, 6*S*), starting from the binary **Complex 2c** and **EI**, we could not obtain any ternary complex corresponding to Pathway C. As can be seen in Scheme 2, when **EI** approaches the thiourea N−H_B, the steric repulsion between **Complex 2c** and **EI** is much stronger than that between **Complex 2a** and **EI**. Accordingly, we started from the binary **Complex 2a** and **EI** for the theoretical calculation on Pathway C.

(30) For the selective theoretical work on the organocatalytic C−C coupling reactions, see: (a) Allemann, C.; Gordillo, R.; Clemente, F. R.; Cheong, P. H.-Y.; Houk, K. N. *Acc. Chem. Res.* **2004**, *37*, 558. (b) Tang, Z.; Jiang, F.; Cui, X.; Gong, L. Z.; Mi, A. Q.; Jiang, Y. Z.; Wu, Y. D. *Proc. Natl. Acad. Sci. U.S.A.* **2004**, *101*, 5755. (c) Clemente, F. R.; Houk, K. N. *Angew. Chem., Int. Ed.* **2004**, *43*, 5766. (d) Cheng, C. L.; Sun, J.; Wang, C.; Zhang, Y.; Wei, S.; Jiang, F.; Wu, Y. D. *Chem. Commun.* **2006**, 215.

(31) (a) Lynch, B. J.; Fast, P. L.; Harris, M.; Truhlar, D. G. *J. Phys. Chem. A* **2000**, *104*, 4811. (b) Yu, Z. X.; Dang, Q.; Wu, Y. D. *J. Org. Chem.* **2001**, *66*, 6029. (c) Zhao, Y.; González-García, N.; Truhlar, D. G. *J. Phys. Chem. A* **2005**, *109*, 2012. (d) Song, J.-W.; Hirosawa, T.; Tsuneda, T.; Hirao, K. *J. Chem. Phys.* **2007**, *126*, 154105. (e) Zhao, Y.; Truhlar, D. G. *Acc. Chem. Res.* **2008**, *41*, 157.

(32) The transition states for the formation of the two byproducts, (5*S*, 6*R*) and (5*S*, 6*S*), along Pathway C are more stable than those along other pathways. The transition state for the byproduct (5*R*, 6*R*) along Pathway C is, however, not the most stable one. Because the transition state for the byproduct (5*R*, 6*R*) is much less stable than those for the other three products, the yield of the byproduct (5*R*, 6*R*) should be extremely low, and thus the diastereoselectivity could not be affected.

(33) This reaction has also been theoretically studied by Pápai et al. (see ref 8d). On the basis of the relative energies of the initial ternary catalyst−nitromethane−chalcone complexes instead of the transition states, they speculated that this reaction may be operated via Pathway B. Because the calculations on the transition states had not been carried out in their work, the validity of the obtained result therein deserves further investigation.

(34) (a) Connon, S. J. *Synlett* **2009**, 354. (b) Tárkányi, G.; Király, P.; Soós, T.; Varga, S. *Chem.-Eur. J.* **2012**, *18*, 1918.

(35) (a) Tárkányi, G.; Király, P.; Varga, S.; Vakulya, B.; Soós, T. *Chem.-Eur. J.* **2008**, *14*, 6078. (b) Király, P.; Soós, T.; Varga, S.; Vakulya, B.; Tárkányi, G. *Magn. Reson. Chem.* **2010**, *48*, 13.
(36) Malerich, J. P.; Hagihara, K.; Rawal, V. H. *J. Am. Chem. Soc.* **2008**, *130*, 14416.
(37) For the selected applications, see: (a) Zhu, Y.; Malerich, J. P.; Rawal, V. H. *Angew. Chem., Int. Ed.* **2010**, *49*, 153. (b) Qian, Y.; Ma, G.; Lv, A.; Zhu, H.-L.; Zhao, J.; Rawal, V. H. *Chem. Commun.* **2010**, *46*, 3004. (c) Konishi, H.; Lam, T. Y.; Malerich, J. P.; Rawal, V. H. *Org. Lett.* **2010**, *12*, 2028. (d) Yang, W.; Du, D.-M. *Org. Lett.* **2010**, *12*, 5450. (e) Yang, W.; Du, D.-M. *Chem. Commun.* **2011**, *47*, 12706. (f) Wang, X.; Yao, W.; Yao, Z.; Ma, C. *J. Org. Chem.* **2012**, *77*, 2959.
(38) Schreiner, P. R. *Chem. Soc. Rev.* **2003**, *32*, 289.